PROCEEDINGS OF SPIE

SPIEDigitalLibrary.org/conference-proceedings-of-spie

Robust eye-safe pulsed fiber laser source for 3D ladar applications

Lars G. Holmen, Gunnar Rustad, Magnus W. Haakestad

Lars G. Holmen, Gunnar Rustad, Magnus W. Haakestad, "Robust eye-safe pulsed fiber laser source for 3D ladar applications," Proc. SPIE 10434, Electro-Optical Remote Sensing XI, 104340N (5 October 2017); doi: 10.1117/12.2278397

SPIE.

Event: SPIE Security + Defence, 2017, Warsaw, Poland

Robust Eye-safe Pulsed Fiber Laser Source for 3D Ladar Applications

Lars G. Holmen[1,2,*], Gunnar Rustad[1], and Magnus W. Haakestad[1,2]

[1]Norwegian Defence Research Establishment, P.O. Box 25, NO-2027 Kjeller, Norway
[2]Dept. of Technology Systems, University of Oslo, P.O. Box 70, NO-2027 Kjeller, Norway

ABSTRACT

We present a pulsed all-fiber Er/Yb-doped master oscillator power amplifier at 1.55 µm wavelength. In a simple two-stage amplifier design, the source delivers 140 µJ pulses at 25 kHz and 50 kHz pulse repetition frequency, and 100 µJ at 100 kHz, with pulse durations of ∼10 ns and beam quality of $M^2 = 1.3$. The MOPA is suitable as a robust field source for ladar applications, and has been tested in an in-house developed scanning ladar system.

Keywords: Erbium fiber laser, ladar, all-fiber

1. INTRODUCTION

Ladar (laser detection and ranging) systems are finding important applications within 3D imaging for use in e.g. autonomous vehicles, topographic mapping and remote sensing. The capabilities of a given ladar system is to a large extent determined by the performance of the laser source, and advances in laser technology enable new designs and applications. In particular, fiber laser technology has driven the power scaling necessary to develop sources for high-performance scanning ladar systems with several kilometer detection ranges. Such ladar systems require several tens of µJ laser pulse energy at several tens of kHz pulse repetition frequency (PRF) with nanosecond pulse duration and good beam quality. Desirable from an applications point of view, fiber lasers can be realized in robust "all-fiber" designs, where all components are fused or spliced together. Such lasers are well protected against mechanical perturbations under harsh operating condition because they are insensitive to optical misalignment.

Pulsed laser sources with a wavelength of 1.55 µm are attractive for remote sensing applications – since this is considered to be an "eye-safe" wavelength. Also, the mature technology of erbium-doped fiber lasers and fiber optic telecommunication has made high-quality components at this wavelength readily available. A common implementation of pulsed fiber laser sources is as "master oscillator power amplifiers" (MOPAs), due to the power scalability and flexibility in seeding conditions. By using gain switched diode lasers as the seed, a particularly high operational flexibility can be obtained, since PRF, pulse duration and pulse shape can be directly controlled through current modulation.

A number of 1.5 µm fiber lasers reaching several hundred µJ pulse energies have been reported, however for pulse durations above 100 ns,[1,2] with poor beam qualities[3] or with less desirable free-space optics in the final amplification stages.[4] An all-fiber MOPA producing 100 µJ, 5 ns, 100 kHz pulses in a diffraction limited beam has been demonstrated,[5] however from a highly complex system consisting of five stages of amplification. A simpler two-stage MOPA was recently reported,[6] but the output suffered from high levels of amplified spontaneous emission (ASE).

We here present a robust all-fiber MOPA at 1.55 µm delivering up to 140 µJ pulse energy at 25 kHz and 50 kHz pulse repetition frequency in a near diffraction limited beam. By seeding with a high power distributed feedback (DFB) laser diode, we are able to use a simple design of only two stages of amplification – a considerably reduced complexity compared to reported fiber lasers of similar performance. The combination of high optical performance and a compact design makes it an attractive source for practical applications such as remote sensing, and we present first results from integrating the MOPA into a scanning ladar system.

*Corresponding author. Email: Lars.Holmen@ffi.no

Electro-Optical Remote Sensing XI, edited by Gary Kamerman, Ove Steinvall,
Proc. of SPIE Vol. 10434, 104340N · © 2017 SPIE · CCC code:
0277-786X/17/$18 · doi: 10.1117/12.2278397

2. EXPERIMENTAL SETUP

2.1 Laser design

The laser design is illustrated in Figure 1. The master oscillator is a DFB diode generating square pulses of 15 ns duration with a peak power of 100 mW at 1550 nm wavelength. This high-power seed source allows us to reach sufficient pulse energies to saturate the power amplifier after a single stage of preamplification, while providing high operational flexibility from being directly current-driven. The preamplifier consists of 7.5 m Er-doped fiber (Liekki Er16-8/125), which is core-pumped at 976 nm with a grating-stabilized diode laser. The pump diode delivers 900 mW from a single mode (SM) fiber, and is combined with the seed signal in a fused wavelength-division multiplexer (WDM). A bandpass filter with a 3 dB bandwidth of 5 nm is used between the amplification stages to prevent out-of-band ASE from entering the power amplifier. A fiber-coupled isolator is also included to protect the preamplifier and seed diode from backward feedback. The signal between the stages is monitored using a fused coupler with a 1:99 coupling ratio.

The power amplifier consists of a mode field adapter, a cladding power stripper and 3 m of Er/Yb-codoped large mode area fiber (Nufern LMA-EYDF-25P/300-He), which is cladding pumped by a multi mode (MM) diode laser delivering up to 40 W at 940 nm. The gain fiber is coiled onto an aluminum cylinder with 4 cm diameter to improve heat dissipation and suppress higher order spatial modes. We use a counter-propagating pump scheme in order to reduce the effective length for unwanted nonlinear processes. Also, by pumping at 940 nm, the requirement for pump wavelength stabilization is relaxed compared to when pumping at the sharp 976 nm Yb absorption peak. Finally, the output fiber is terminated with an 8° angle cleave to suppress feedback.

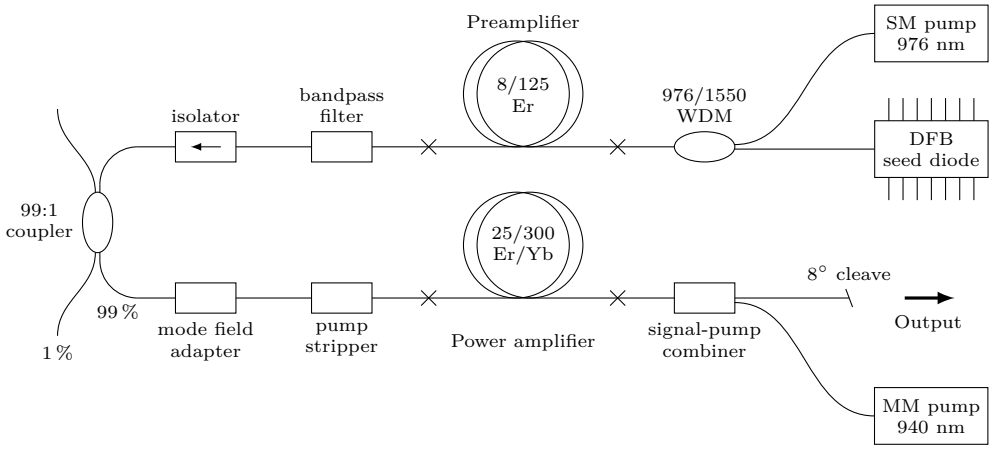

Figure 1. Schematic design of the two-stage all-fiber master-oscillator power-amplifier. Abbreviations are explained in the text.

2.2 ASE characterization

A free-space acousto-optic modulator (AOM) is used to deflect part of the output beam into the first order of diffraction in order to time-gate the laser output. The beam deflection is synchronized to the laser pulses, and the time windows are chosen to contain either only the pulses, or only the ASE signal between pulses. By comparing the average power in the deflected beam in these two cases, the fraction of the total average power contained in the pulses is determined, and hence the pulse energies. The AOM setup also enables measurements of optical spectra for the pulses and background ASE separately.

3. RESULTS AND DISCUSSION

The square seed pulses have a peak power of 100 mW, which corresponds to a pulse energy of 1.5 nJ. Without accounting for losses in various fiber components in the MOPA, this means for instance that a total gain of 48 dB is needed to reach 100 µJ output pulse energy. After the first amplifier stage, we measured the average signal power to 87 mW at 25 kHz pulse repetition frequency, 130 mW at 50 kHz and 180 mW at 100 kHz. The pulse shape is only weakly altered in the preamplifier with respect to the seed.

3.1 Output power

The average output power from the MOPA was measured at 25, 50 and 100 kHz pulse repetition frequencies (PRFs), and is shown in Figure 2(a). Temporal pulse traces for a selection of the output powers at 50 kHz are shown in Figure 2(b). The instantaneous power during the pulses has been estimated from the areas below the pulse traces, scaled to the pulse energies that are determined in Section 3.3. We observe that the output power is nearly independent of PRF except for a weak roll-off for operation at 25 and 50 kHz. At these PRFs, the maximum available pump power (40 W) was not used due to the onset of unstable output with significant pulse-to-pulse fluctuations caused by parasitic lasing. For both PRFs, the fluctuations appeared to emerge at roughly the same pulse energy of 135 µJ, in other words at the same level of inversion in the gain fiber. When operating at 100 kHz, the output is currently pump limited.

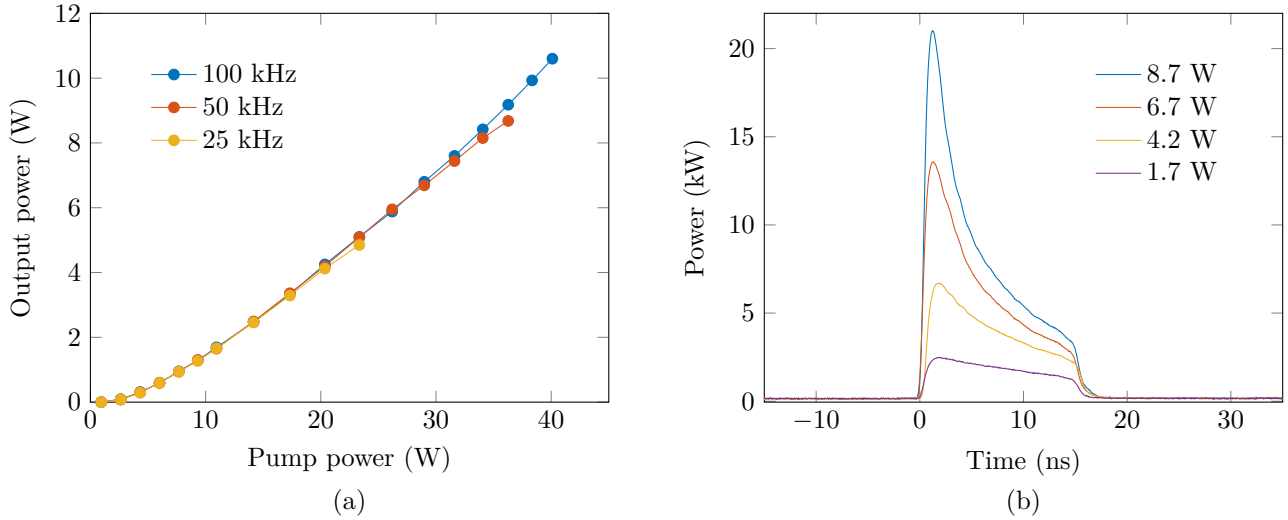

Figure 2. Average power from the MOPA for operation at different pulse repetition frequencies (a), and temporal pulse profiles for 50 kHz operation (b). The legend indicates the corresponding average output power.

Compared to the 15 ns square pulses used to seed the laser, the pulses in Figure 2(b) are deformed due to dynamic gain saturation in the power amplifier, where the leading edge of the pulse is strongly amplified and depletes the gain for the trailing edge. In the case of the highest output power of 8.7 W at 50 kHz, we measure the FWHM pulse duration to be 4 ns. Although the effective pulse shortening can be desirable in certain applications, the peak power increases to undesirable large values that causes unwanted nonlinear effects. We estimate the peak power of these pulses to ∼20 kW, which is far into the regime where nonlinear processes have been encountered in similar fiber amplifiers.[5,7] A way to circumvent these saturation effects is through seed pulse shaping, which has been demonstrated in a number fiber MOPAs.[8,9]

3.2 Beam quality

We determined the beam quality (M^2) of the MOPA from second moments of near- and far-field beam profiles, as those shown in Figure 3. Although a slight content of higher order modes was evident when squeezing the fiber, we measured a near diffraction limited beam quality of $M^2 = 1.3$ in both x and y-direction. We did not observe variations in the beam quality at other output powers and pulse repetition frequencies. Good beam quality is an important feature for long range ladar applications, and the fiber geometry ensures a near symmetrical divergence in different spatial directions.

3.3 Pulse energy and ASE-content

The fraction of the average output power that corresponds to background signal between pulses was measured using an acousto-optic modulator as described in Section 2.2, and the results are shown in Figure 4(a). As expected, the ASE content for a given output power depends strongly on the pulse repetition frequency. Whereas

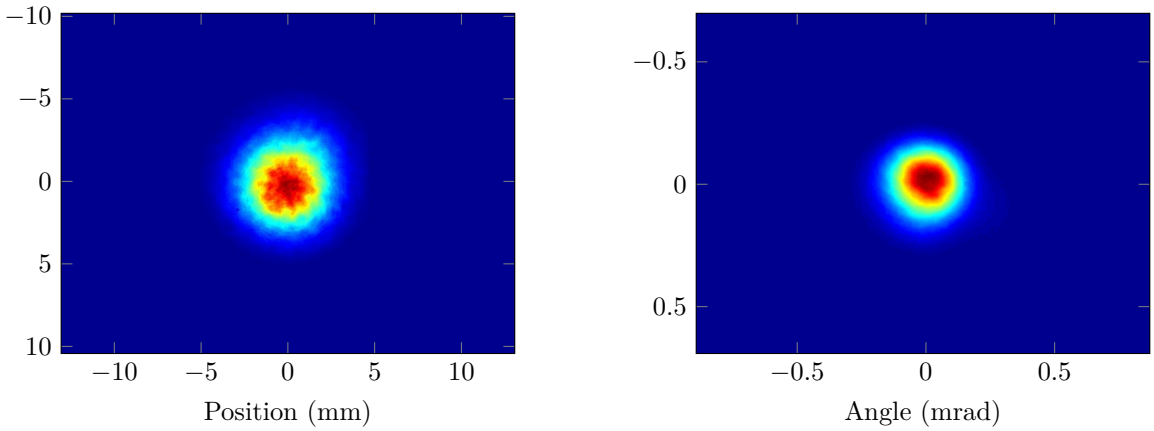

Figure 3. Near-field (left) and far-field (right) beam profiles with 4σ diameters of 7.0 mm and 0.38 mrad, respectively, giving a beam quality of $M^2 = 1.3$. The laser is operated at 50 kHz with 8.7 W output power.

the ASE fraction is around 5 % for the highest output powers at 100 kHz, it is up to 30 % at 25 kHz. Furthermore, we observe a sharp rise in ASE power for both 25 kHz and 50 kHz PRF starting at average output powers around 4 W and 8 W, respectively. At still higher powers, we experienced large pulse-to-pulse fluctuations from the onset of parasitic lasing, which currently sets a limit for power scaling at 25 kHz and 50 kHz. The power thresholds for this effect was found to vary between measurements, which we believe is caused by the high sensitivity to external feedback from the measurement setup.

Having determined the background ASE content, we obtain the pulse energies for different PRFs and output powers shown in Figure 4(b). Also indicated in the figure as dashed lines are the pulse energies expected for the different PRFs in the case of 100 % pulse energy content. The maximum pulse energy obtained is ∼135 µJ before the rapidly increasing background power prevents further scaling. Notably, the pulse energy is limited to the same value at both 25 kHz and 50 kHz, whereas the maximum pulse energy at 100 kHz is 100 µJ, limited by available pump power. With additional pump power we anticipate energy scalability towards 135 µJ also at 100 kHz PRF.

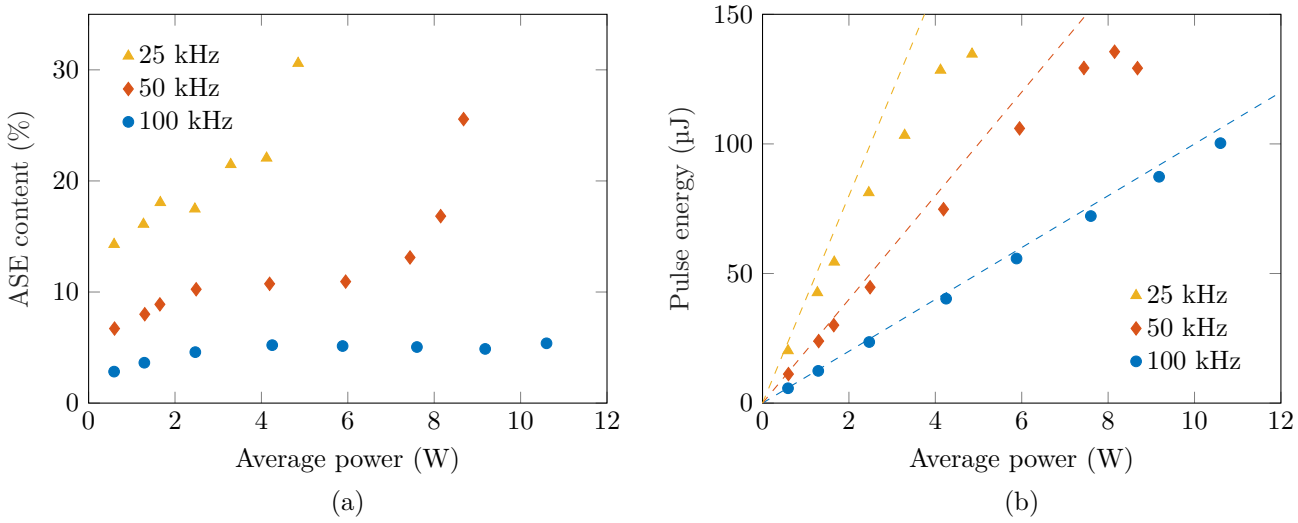

Figure 4. Measured ASE content (a) of the output at different pulse repetition frequencies, and the deduced energies in the corresponding pulses (b). For reference, the dashed lines in (b) indicate the expected pulse energies in the absence of any ASE.

3.4 Spectrum

Figure 5 shows optical spectra of the MOPA measured for different output powers when operating at 50 kHz. The spectra contains both the pulses and ASE, and the 5 nm band-pass filter used between the amplification stages is clearly seen as a pedestal feature. Also evident is a drastic change in spectral appearance when comparing the spectra at 5.6 W and 6.7 W output, where the latter shows symmetric side bands characteristic of modulation instability. This effect is explained as the nonlinear optical process of degenerate four wave mixing (FWM) that is phase matched due to self phase modulation,[10] and is commonly encountered in high peak power fiber lasers operating in the anomalous dispersion regime.[5,7]

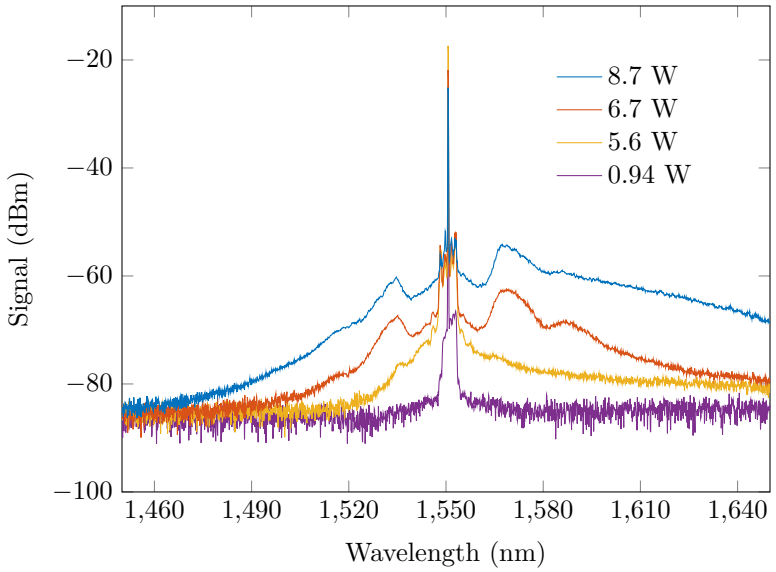

Figure 5. Optical spectra from the MOPA when operating at 50 kHz pulse repetition frequency.

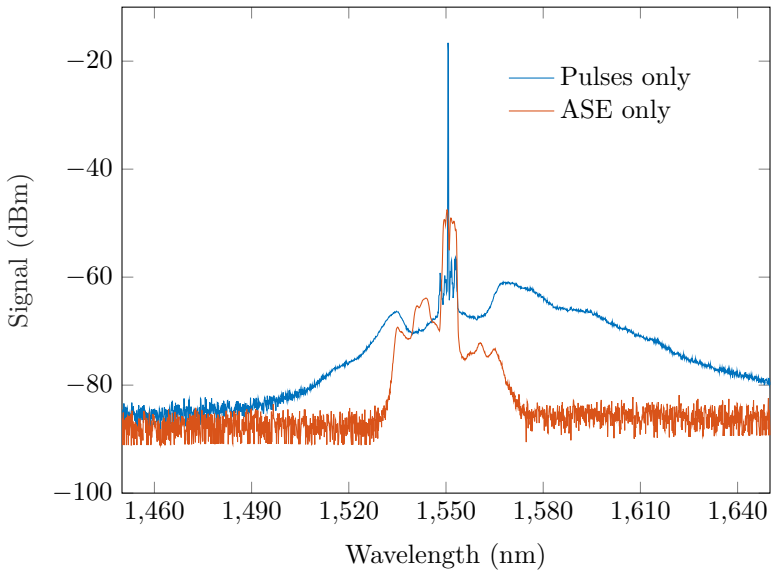

Figure 6. Optical spectra when time gating the output signal to contain only the pulses or the ASE between pulses. The MOPA was operated at 50 kHz pulse repetition frequency and 7.5 W output power.

In order to determine if the spectral broadening is caused mainly by nonlinear effects or background ASE, we time-gated the signal using the AOM-setup described in Section 2.2 to contain only the pulses or only the ASE

between pulses. The measured spectra are shown in Figure 6, and from comparing with Figure 5, we conclude that spectral broadening outside the 5 nm band pass filter is predominantly caused by nonlinear effects. The spectral broadening observed in addition to the FWM side lobes are attributed to an interplay between a variety of dispersive and nonlinear processes.[10,11]

3.5 Ladar

In order to evaluate the MOPA as a laser source for 3D ladar applications, it was integrated into an in-house developed scanning ladar system. A direct measure of laser performance in this particular setup was obtained by measuring the average return signal from a distant target. The detection system includes a detector with ∼50 MHz bandwidth and a band pass filter with 25 nm spectral bandwidth. Since the system is insensitive to background ASE between pulses, only the energy delivered during the pulses and within the filter bandwidth will contribute to the signal. For comparison, we also performed measurements with a commercial pulsed erbium-doped fiber laser from LEA Photonics (PEFL-series, custom made), capable of delivering 5 W average power at 1550 nm at 50-200 kHz pulse repetition frequency with ∼10 ns pulse duration and with good beam quality. Both lasers were operated at 54 kHz during the tests, and the measurements were done within a short time span to reduce the influence of changing atmospheric conditions.

Figure 7 shows the return signal for different output powers, and we observe that the commercial laser gives $5-10\,\%$ higher return signals for a given average output power. This difference may have several explanations, including differences in alignment of ladar optics and changes in atmospheric conditions during the measurements. The pulse energy content of the commercial laser was not characterized in this work, but if the ASE content of this laser is smaller than the ∼10 % measured for our laser, this would also contribute to the slightly larger signal to output power ratio in Figure 7. Nevertheless, the in-house laser can be operated at higher pulse energies, which generally will enable 3D imaging at longer distances or of less scattering targets.

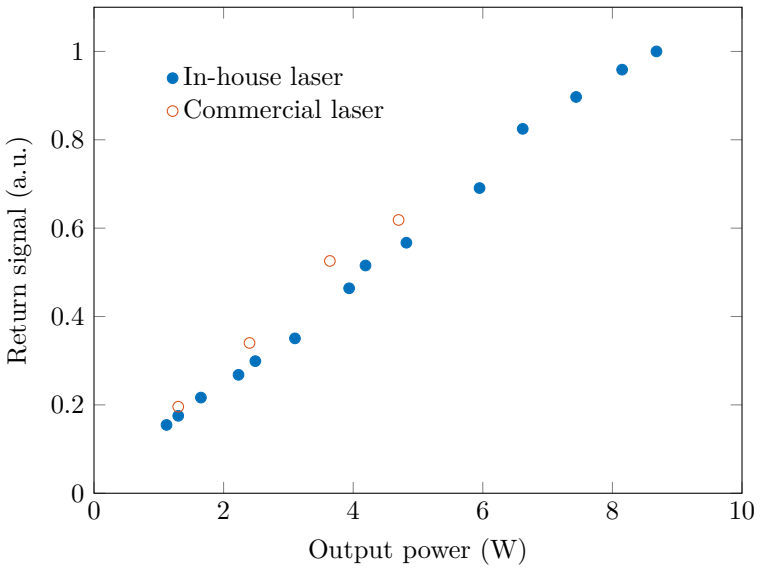

Figure 7. Measured return signal from a distant target after installing the MOPA in a ladar system. Results with a commercial laser are shown for comparison.

Comparing the ladar measurements to the pulse energies in Figure 4(b), we do not observe a significant roll-off in return signal that would be expected for output powers above ∼8 W. The cause of this is currently under investigation, but the ASE content and parasitic lasing processes is highly sensitive to external feedback, which may have differed in the lab- and field measurements. Also, the repetition frequency was slightly higher than 50 kHz, which can have pushed the sharp rise in ASE content to higher output powers.

4. CONCLUSIONS

In conclusion, we demonstrate a diode-seeded pulsed all-fiber MOPA at 1.55 µm. The amplifier delivers pulse energies up to 140 µJ at 25 and 50 kHz pulse repetition frequencies, limited by amplified spontaneous emission, and 100 µJ at 100 kHz, limited by pump power. The pulse durations range from 4 to 15 ns (FWHM) depending on gain saturation, and the beam quality is $M^2 = 1.3$. Our two-stage amplifier design delivers high performance while maintaining a low system complexity. Combined with a robust all-fiber implementation, the MOPA is well suited as a versatile field source for remote sensing applications and 3D imaging, and it has been used with success in an in-house developed scanning ladar system.

ACKNOWLEDGMENTS

The authors thank Gunnar Arisholm, Stig Landrø and Øystein Farsund for technical assistance during the ladar-measurements.

REFERENCES

[1] Kotov, L., Likhachev, M., Bubnov, M., Medvedkov, O., Lipatov, D., Guryanov, A., Zaytsev, K., Jossent, M., and Fevrier, S., "Millijoule pulse energy 100-nanosecond Er-doped fiber laser," *Optics Letters* **40**(7), 1189–1192 (2015).

[2] Nicholson, J. W., DeSantolo, A., Yan, M. F., Wisk, P., Mangan, B., Puc, G., Yu, A. W., and Stephen, M. A., "High energy, 1572.3 nm pulses for CO_2 LIDAR from a polarization-maintaining, very-large-mode-area, Er-doped fiber amplifier," *Optics Express* **24**(17), 19961–19968 (2016).

[3] Desmoulins, S. and Teodoro, F., "High-gain Er-doped fiber amplifier generating eye-safe MW peak-power, mJ-energy pulses," *Optics Express* **16**(4), 2431–2437 (2008).

[4] Zhao, Z., Xuan, H., Igarashi, H., Ito, S., Kakizaki, K., and Kobayashi, Y., "Single frequency, 5 ns, 200 µJ, 1553 nm fiber laser using silica based Er-doped fiber," *Optics Express* **23**(23), 29764–29771 (2015).

[5] Pavlov, I., Dülgergil, E., Ilbey, E., and Ilday, F. Ö., "Diffraction-limited, 10-W, 5-ns, 100-kHz, all-fiber laser at 1.55 µm," *Optics Letters* **39**(9), 2695–2698 (2014).

[6] Dvoyrin, V. V., Klimentov, D., Klepsvik, J. O., Mazaeva, I. V., and Sorokina, I. T., "Multi-kilowatt peak power nanosecond Er-doped fiber laser," *IEEE Photonics Technology Letters* **28**(23), 2772–2775 (2016).

[7] Guo, K., Wang, X., Zhou, P., and Shu, B., "4 kW peak power, eye-safe all-fiber master-oscillator power amplifier employing Yb-free Er-doped fiber," *Applied Optics* **54**(3), 504–508 (2015).

[8] Schimpf, D. N., Ruchert, C., Nodop, D., Limpert, J., Tünnermann, A., and Salin, F., "Compensation of pulse-distortion in saturated laser amplifiers.," *Optics Express* **16**(22), 17637–17646 (2008).

[9] Sobon, G., Kaczmarek, P., Antonczak, A., Sotor, J., Waz, A., and Abramski, K., "Pulsed dual-stage fiber MOPA source operating at 1550 nm with arbitrarily shaped output pulses," *Applied Physics B: Lasers and Optics* **105**(4), 721–727 (2011).

[10] Agrawal, G. P., [*Nonlinear fiber optics*], Academic press (2013).

[11] Abeeluck, A. K. and Headley, C., "Continuous-wave pumping in the anomalous- and normal-dispersion regimes of nonlinear fibers for supercontinuum generation," *Optics Letters* **30**(1), 61–63 (2005).